

Reactivity of Five-Coordinate Intermediate Generated by Laser Photolysis of Monoligated Chloro(5,10,15,20-tetraphenylporphinato)chromium(III) in Toluene

Masahiko Inamo, Mikio Hoshino,[†] Kiyohiko Nakajima, Sen-ichi Aizawa,^{††} and Shigenobu Funahashi^{*,††}

Faculty of Education, Aichi University of Education, Kariya 448

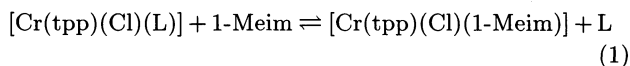
[†]The Institute of Physical and Chemical Research, Wako 351-01

^{††}Laboratory of Analytical Chemistry, Faculty of Science, Nagoya University, Nagoya 464-01

(Received March 6, 1995)

The Cr(III) porphyrin complexes [Cr(tpp)(Cl)(H₂O)] (**1**) and [(Cr(tpp)(Cl)(py))] (**2**) (tpp represents the dianion of 5,10,15,20-tetraphenylporphine) crystallized from a chloroform–toluene mixture in the tetragonal space group *I*₄, *Z*=2, *a*=13.559(5), *b*=13.559(5), *c*=9.770(3) Å, *V*=1796(3) Å³, and from a dichloroethane–toluene mixture containing a small amount of pyridine (py) in the monoclinic space group *P*2₁/*n*, *Z*=4, *a*=14.655(5), *b*=23.498(4), *c*=13.152(2) Å, *β*=101.54(1)°, *V*=4437(2) Å³, respectively. The axial Cr–O bond length for **1** and the axial Cr–N bond length for **2** are 2.239(3) and 2.140(5) Å, respectively. Laser irradiation of the toluene solution of [Cr(tpp)(Cl)(L)] causes the photodissociation of the axial ligand L, where L represents H₂O or 3-cyanopyridine, to give the five-coordinate intermediate [Cr(tpp)(Cl)]. The rate constant of the axial ligand recombination reaction falls into a narrow range around 1×10⁹ mol^{−1} kg s^{−1} at 25.0 °C for both reactions. The activation parameters indicate the very high reactivity of the five-coordinate intermediate. The diffusion-controlled process is regarded as a rate-determining step for the recombination.

Much attention has been focused on the metalloporphyrins because of their importance in biological functions such as oxygen transport and storage in hemoproteins. It is well known that porphyrin ligands offer very characteristic features to the metal complexes with respect to their chemical reactivity as compared with other complexes having non-macrocyclic ligands. One of the most surprising chemical phenomena caused by the porphyrin ligand is a labilizing effect on the substitution reaction of the complex at its axial coordination site in solution. This effect amounts to several orders of magnitude in rate for some metalloporphyrins, especially for those of chromium(III),^{1,2)} cobalt(III),³⁾ and rhodium(III)⁴⁾ ions which are usually substitution inert. Mechanistic studies have been done in order to elucidate the cause of labilizing effects. Recently, we have reported the equilibria and kinetics for the axial substitution reaction of monoligated chloro(5,10,15,20-tetraphenylporphinato)chromium(III) ([Cr(tpp)(Cl)(L)]) by 1-methylimidazole (1-Meim) in toluene from the viewpoint of the substituent effect of the leaving ligand L:



where L represents pyridine and several substituted pyridines.^{2b)} It has been concluded that the substitution reaction proceeds via a limiting dissociative mechanism and that the five-coordinate species [Cr(tpp)(Cl)] can be assumed to be a reactive intermediate. It is, however, difficult to obtain solid evidence to support this mechanism, since such intermediate species are usually too reactive to be detected by conventional spectrophotometric methods.

Natural and synthetic metalloporphyrins are known to undergo photodissociation of the axial ligand upon laser irradiation in solution.^{5–8)} It has been demonstrated that laser irradiation of [Cr(tpp)(Cl)(py)] in acetone produces the five-coordinate complex [Cr(tpp)(Cl)].⁷⁾ Laser photolysis may, therefore, be a useful method to investigate the reactivity of the five-coordinate complex which is regarded as an intermediate in the axial ligand substitution reaction. The purpose of the present study is to characterize the five-coordinate intermediate produced by means of laser photolysis and to elucidate the axial labilizing effect by comparing the reactivity of the five-coordinate intermediate with the kinetic behavior for the axial substitution in reaction 1 previously obtained.^{2b)} Toluene was used as an inert sol-

vent in order to avoid the complexity caused by solvent coordination to the central metal ion.

Experimental

Reagents. Chloro(5,10,15,20-tetraphenylporphinato)-chromium(III) was prepared and purified according to the reported procedure.⁹ Crystals of $[\text{Cr}(\text{tpp})(\text{Cl})(\text{H}_2\text{O})]$ (**1**) were obtained by the following procedure. Thirty mg of the Cr(III)-tpp complex was dissolved in 1 cm³ of hot chloroform and an equal amount of toluene was added to the solution. The mixture was filtered, then the filtrate was set aside in the dark for several days, allowing the slow evaporation of the solvent. The precipitated purple crystalline product was collected via filtration and dried in vacuo at room temperature for several hours. Crystals of $[\text{Cr}(\text{tpp})(\text{Cl})(\text{py})]$ (**2**) were prepared by the same procedure as described above, using 1 cm³ of dichloroethane containing 30 mg of pyridine instead of chloroform. 3-Cyanopyridine was purified by recrystallization from a mixture of *o*-xylene and hexane. Toluene was dried over sodium and then distilled.

Measurements. UV-visible absorption spectra were recorded on a Hitachi U-3000 spectrophotometer. Laser photolysis was carried out by using a Nd-YAG laser (Surelite, Continuum) equipped with second (532 nm) and third (355 nm) harmonic generators. The transients were monitored by a detection system (TSP-601, Unisoku, Japan). The laser pulse width was 6 ns. The intensity of an analyzing light beam from a xenon lamp (L2195, Hamamatsu Photonics) passed through a sample cell was measured by a photomultiplier (R2949, Hamamatsu Photonics) attached to a monochromator. Experimental pseudo-first-order rate constants k_{obsd} were obtained from non-linear least-squares analyses for absorbance decay curves after laser irradiation. An estimated standard deviation of the mean of several measurements of k_{obsd} was less than $\pm 3\%$. The concentration of water in the toluene solution was determined by the Karl-Fischer titrator (CA-06, Mitsubishi Kasei).

X-Ray Structure Analysis. X-Ray diffraction experiments were performed on a Rapid X-Ray Diffraction Image Processor (DIP320N, MAC Science Co., Ltd.) for **1** and a Rigaku AFC-5R diffractometer for **2**, using graphite monochromated Mo $K\alpha$ radiation ($\lambda = 0.71073 \text{ \AA}$) at ambient temperature. Suitable reflections (8213) for **1** were collected by using continuous 30 Weissenberg photographs with a ϕ range of 6° (total ϕ range, $0 - 180^\circ$), and 11089 reflections for **2** using the $\theta-2\theta$ scan method (scan range, $1.42 + 0.5 \tan \theta$; $2\theta_{\text{max}}$, 60°). Empirical absorption corrections were performed for **2** based on ψ -scan data. The structures were solved by the direct method using MULTAN78¹⁰ for **1** and SHELXS-86¹¹ for **2**. All calculations were carried out using Crystan-G¹² for **1** and UNICS-III¹³ for **2**. Atomic scattering factors and anomalous dispersion terms were taken from Ref. 14. Non-hydrogen atoms were refined anisotropically, and hydrogen atoms for **1** were placed in the observed positions and held invariant, while those for **2** were included in the calculated positions. The crystallographic data are summarized in Table 1. Tables of anisotropic thermal parameters for non-hydrogen atoms and observed and calculated structure factors are deposited as Document No. 68035 at the Office of the Editor of Bull. Chem. Soc. Jpn.

Results

Crystal and Molecular Structures of $[\text{Cr}(\text{tpp})(\text{Cl})(\text{H}_2\text{O})]$ (1**) and $[\text{Cr}(\text{tpp})(\text{Cl})(\text{py})]$ (**2**).** Recrystallizations of the Cr(III)-tpp complexes, **1** and **2**, from the chloroform-toluene and dichloroethane-toluene mixture, respectively, gave single crystals suitable for X-ray diffraction measurements. The perspective views of **1** and **2** are displayed in Figs. 1 and 2, respectively, along with the atomic numbering schemes. The selected bond distances and angles for **1** and **2** are listed in Table 2. Atomic positional parameters are given in Table 3. The porphyrin molecule in **1** has a C_4 axis passing through the Cl, Cr, and O atoms, and the peripheral phenyl groups are almost perpendicular to the porphyrin plane with a dihedral angle of 89.35° between the phenyl ring and the mean porphyrinato plane defined by four pyrrole nitrogens. The porphyrinato core has no ruffling and consequently the symmetry of the porphyrin molecule is extremely high. The

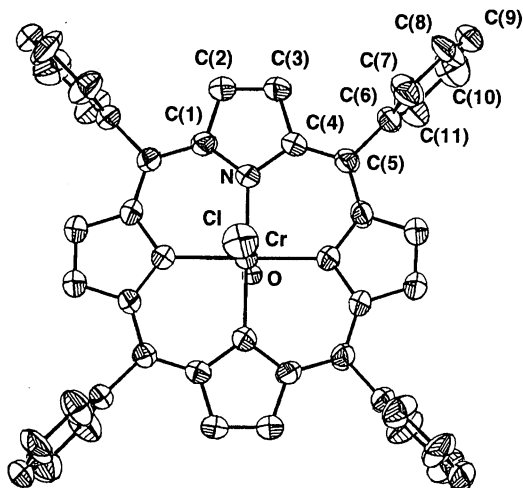


Fig. 1. Molecular structure of $[\text{Cr}(\text{tpp})(\text{Cl})(\text{H}_2\text{O})]$ (**1**) showing 50% probability ellipsoids. Hydrogen atoms are omitted for clarity.

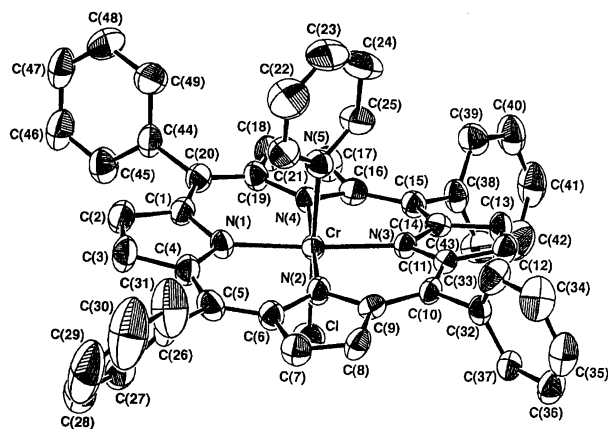


Fig. 2. Molecular structure of $[\text{Cr}(\text{tpp})(\text{Cl})(\text{py})]$ (**2**) showing 50% probability ellipsoids. Hydrogen atoms are omitted for clarity.

Table 1. Crystallographic Data for [Cr(tpp)(Cl)(H₂O)] (**1**) and [Cr(tpp)(Cl)(py)] (**2**)

| Complex | 1 | 2 |
|---|---|--|
| Formula | CrClON ₄ C ₄₄ H ₃₀ | CrClN ₅ C ₄₉ H ₃₃ |
| FW | 718.2 | 779.3 |
| Color, habit | Purple, rhombic | Purple, rhombic |
| Cryst. size/mm | 0.42×0.30×0.28 | 0.50×0.20×0.20 |
| Cryst. syst. | Tetragonal | Monoclinic |
| Space group | <i>I</i> 4 | <i>P</i> 2 ₁ / <i>n</i> |
| Temp/K | 296—298 | 296—298 |
| Unit cell dimens <i>a</i> /Å | 13.559(5) | 14.655(5) |
| <i>b</i> /Å | 13.559(5) | 23.498(4) |
| <i>c</i> /Å | 9.770(3) | 13.152(2) |
| β /° | | 101.54(1) |
| Volume/Å ³ | 1796(3) | 4437(2) |
| <i>Z</i> | 2 | 4 |
| <i>F</i> (000) | 742 | 1612 |
| <i>d</i> _{calcd} /g cm ⁻³ | 1.33 | 1.17 |
| Radiation; λ /Å | Mo <i>K</i> α ; 0.71073 | Mo <i>K</i> α ; 0.71073 |
| Refins. measd | $\pm h \pm k \pm l$ | $+h + k \pm l$ |
| No. of refins. measd | 8213 | 11089 |
| Criterion for obsn | $F_o > 3\sigma(F_o)$ | $F_o > 6\sigma(F_o)$ |
| No. of refins. used | 1147 | 4080 |
| Int <i>R</i> | 0.05 | 0.01 |
| μ /cm ⁻¹ | 3.87 | 3.47 |
| Abs correction | None | 0.897—0.999 (Transm coeff) |
| <i>R</i> ^{a)} | 0.0547 | 0.0649 |
| <i>R</i> _w ^{b)} | 0.0651 | 0.0828 |
| <i>w</i> | $(\sigma(F_o)^2 + (0.02F_o)^2)^{-1}$ | $(\sigma(F_o)^2 + (0.02F_o)^2)^{-1}$ |
| Test of chirality | None | None |

a) $\Sigma ||F_o| - |F_c|| / \Sigma |F_o|$. b) $[\Sigma w(|F_o| - |F_c|)^2 / \Sigma w|F_o|^2]^{1/2}$.Table 2. Selected Bond Lengths (Å) and Angles (deg) for **1** and **2**

| 1 | | 2 | | | |
|--------------|----------|--------------|----------|--------------|----------|
| Bond lengths | | | | | |
| Cr—Cl | 2.242(3) | Cr—Cl(1) | 2.311(2) | Cr—N(1) | 2.031(5) |
| Cr—O | 2.239(3) | Cr—N(2) | 2.021(6) | Cr—N(3) | 2.037(5) |
| Cr—N | 2.031(2) | Cr—N(4) | 2.015(6) | Cr—N(5) | 2.140(5) |
| Bond angles | | | | | |
| Cl—Cr—O | 180.0 | Cl—Cr—N(1) | 92.8(2) | Cl—Cr—N(2) | 93.1(2) |
| Cl—Cr—N | 89.0(1) | Cl—Cr—N(3) | 91.0(2) | Cl—Cr—N(4) | 90.2(2) |
| O—Cr—N | 91.0(1) | Cl—Cr—N(5) | 177.7(2) | N(1)—Cr—N(2) | 89.3(2) |
| | | N(1)—Cr—N(3) | 176.2(2) | N(1)—Cr—N(4) | 90.5(2) |
| | | N(1)—Cr—N(5) | 88.6(2) | N(2)—Cr—N(3) | 90.3(2) |
| | | N(2)—Cr—N(4) | 176.7(2) | N(2)—Cr—N(5) | 88.7(2) |
| | | N(3)—Cr—N(4) | 89.8(2) | N(3)—Cr—N(5) | 87.6(2) |
| | | N(4)—Cr—N(5) | 87.9(2) | | |

pyrrole rings are almost coplanar with the porphinato plane with a dihedral angle of 2.7° between the mean porphinato plane and the C(1)—N(1)—C(4) plane. The chlorine and oxygen atoms are coordinated in axial positions with similar bond distances ($r(\text{Cr—Cl})=2.242(3)$ Å and $r(\text{Cr—O})=2.239(3)$ Å). The central chromium atom is displaced by 0.035(4) Å from the mean plane defined by four pyrrole nitrogens toward the axial oxygen atom. The intermolecular interactions between the

phenyl rings or porphyrin rings are not observed in the crystal of **1**. The four Cr—N distances (2.031(2) Å) are the same, due to the crystallographic symmetry.

In the case of the molecule of **2**, the pyridine plane is within experimental error perpendicular to the N₄-plane (dihedral angle 89.9(2)°). A dihedral angle between the pyridine plane and the plane defined by the Cl, N(5), C(5), and C(15) atoms is 3.7(2)° and the α -carbon atoms of the pyridine ligand are almost directly

Table 3. Atomic Coordinates ($\times 10^4$) and Isotropic Thermal Parameters

| Atom | <i>x</i> | <i>y</i> | <i>z</i> | $B_{\text{eq}}^{\text{a}}/\text{\AA}^2$ | Atom | <i>x</i> | <i>y</i> | <i>z</i> | $B_{\text{eq}}^{\text{a}}/\text{\AA}^2$ |
|---------------------------------|-----------|-----------|-----------|---|-------|----------|----------|-----------|---|
| [Cr(tpp)(Cl)(H ₂ O)] | | | | | C(13) | 58(5) | 4252(3) | 6120(5) | 3.2 |
| Cr | 0 | 0 | 1608 | 2.82 | C(14) | 669(5) | 3797(3) | 6551(5) | 2.9 |
| Cl | 0 | 0 | −687(3) | 5.94 | C(15) | 1362(5) | 3547(3) | 6087(5) | 2.8 |
| O | 0 | 0 | 3899(3) | 1.82 | C(16) | 1817(4) | 3046(3) | 6409(5) | 3.0 |
| N | 1451(2) | 374(1) | 1572(5) | 3.49 | C(17) | 2442(5) | 2746(3) | 5878(5) | 4.0 |
| C(1) | 2238(2) | −261(2) | 1611(5) | 3.54 | C(18) | 2663(5) | 2248(3) | 6367(5) | 4.0 |
| C(2) | 3150(2) | 294(2) | 1615(7) | 4.20 | C(19) | 2199(5) | 2237(3) | 7233(5) | 3.2 |
| C(3) | 2901(2) | 1261(2) | 1623(8) | 4.19 | C(20) | 2311(5) | 1809(3) | 7986(5) | 3.4 |
| C(4) | 1835(2) | 1317(2) | 1612(4) | 3.52 | C(21) | −513(6) | 2106(3) | 8240(6) | 4.6 |
| C(5) | 1296(2) | 2192(2) | 1608(6) | 3.57 | C(22) | −1285(7) | 1780(4) | 7799(8) | 7.1 |
| C(6) | 1849(2) | 3147(2) | 1652(6) | 3.76 | C(23) | −1630(6) | 1811(4) | 6749(7) | 6.3 |
| C(7) | 2119(4) | 3607(4) | 407(8) | 5.6 | C(24) | −1225(6) | 2170(4) | 6175(6) | 6.1 |
| C(8) | 2645(5) | 4485(4) | 440(10) | 6.7 | C(25) | −456(5) | 2499(3) | 6657(6) | 4.3 |
| C(9) | 2925(2) | 4898(2) | 1580(10) | 5.7 | C(26) | 813(6) | 2258(3) | 11885(5) | 4.8 |
| C(10) | 2667(6) | 4463(4) | 2834(8) | 6.3 | C(27) | 1678(8) | 2219(4) | 12688(6) | 6.4 |
| C(11) | 2106(5) | 3573(4) | 2827(8) | 5.9 | C(28) | 1560(11) | 2007(5) | 13659(6) | 10.6 |
| [Cr(tpp)(Cl)(py)] | | | | | C(29) | 673(12) | 1873(5) | 13814(8) | 12.0 |
| Cr | 1052.2(7) | 2978.5(5) | 8392.0(8) | 2.5 | C(30) | −61(10) | 1932(5) | 13086(10) | 11.3 |
| Cl | 2321(1) | 3537(1) | 9088(1) | 3.9 | C(31) | −17(7) | 2116(5) | 12076(8) | 7.7 |
| N(1) | 1566(4) | 2294(2) | 9263(4) | 2.9 | C(32) | −1304(5) | 4435(3) | 8673(5) | 3.0 |
| N(2) | 344(4) | 3204(2) | 9499(4) | 2.9 | C(33) | −2223(5) | 4292(3) | 8531(6) | 4.4 |
| N(3) | 460(3) | 3635(2) | 7483(4) | 2.5 | C(34) | −2881(6) | 4698(4) | 8722(7) | 5.7 |
| N(4) | 1697(4) | 2724(2) | 7253(4) | 2.6 | C(35) | −2588(6) | 5226(4) | 9081(6) | 5.2 |
| N(5) | −114(4) | 2470(2) | 7686(4) | 3.3 | C(36) | −1693(6) | 5384(3) | 9196(6) | 4.4 |
| C(1) | 2044(5) | 1847(3) | 8938(5) | 3.1 | C(37) | −1021(5) | 4993(3) | 8992(5) | 3.7 |
| C(2) | 2221(6) | 1421(3) | 9750(5) | 4.2 | C(38) | 1620(5) | 3856(3) | 5184(5) | 3.4 |
| C(3) | 1864(6) | 1621(3) | 10561(6) | 4.5 | C(39) | 1380(5) | 3662(3) | 4163(5) | 4.0 |
| C(4) | 1444(5) | 2160(3) | 10246(5) | 3.5 | C(40) | 1658(6) | 3958(4) | 3371(6) | 4.8 |
| C(5) | 928(5) | 2493(3) | 10839(5) | 3.6 | C(41) | 2176(6) | 4432(4) | 3572(6) | 5.3 |
| C(6) | 438(5) | 2980(3) | 10486(5) | 3.2 | C(42) | 2417(7) | 4642(4) | 4560(7) | 5.8 |
| C(7) | −93(5) | 3316(3) | 11069(5) | 3.8 | C(43) | 2136(6) | 4361(3) | 5379(6) | 5.0 |
| C(8) | −551(5) | 3723(3) | 10430(5) | 3.4 | C(44) | 2776(5) | 1267(3) | 7730(5) | 3.6 |
| C(9) | −278(4) | 3656(3) | 9437(5) | 2.7 | C(45) | 3664(5) | 1117(3) | 8188(6) | 4.6 |
| C(10) | −582(4) | 3999(3) | 8569(5) | 2.5 | C(46) | 4069(6) | 609(4) | 7937(7) | 5.3 |
| C(11) | −237(4) | 3982(3) | 7656(5) | 2.6 | C(47) | 3554(6) | 237(3) | 7228(6) | 4.9 |
| C(12) | −505(5) | 4361(3) | 6800(5) | 3.3 | C(48) | 2673(7) | 383(3) | 6779(7) | 6.7 |
| | | | | | C(49) | 2268(6) | 889(4) | 7015(6) | 5.6 |

a) The equivalent isotropic displacement parameter B_{eq} is calculated as: $B_{\text{eq}} = (4/3) \sum_i \sum_j \beta_{ij} a_i \cdot a_j$.

above the line defined by the C(5) and C(15) atoms (see Fig. 2). The Cl atom and N atom of the pyridine ligand are coordinated in axial positions with bond distances of $r(\text{Cr}-\text{Cl}) = 2.311(2)$ Å and $r(\text{Cr}-\text{N}(5)) = 2.140(5)$ Å. The central chromium atom is displaced by $0.063(2)$ Å from the mean plane defined by four pyrrole nitrogens toward the axial Cl atom. The four equatorial Cr–N distances ($2.031(5)$, $2.021(6)$, $2.037(5)$, and $2.015(6)$ Å) are close to each other. In Fig. 3 are given the perpendicular displacements of each atom from the mean plane of the 24-atom core for the molecule **2** which has a pronounced quasi-S₄ ruffling. The magnitude of the ruffling is not exceptional for porphyrin derivatives.¹⁵⁾ Dihedral angles between the peripheral phenyl groups and the mean plane of the 24-atom core are within the normal range with values of 59.0, 78.9, 69.7, and 72.1°.

Photoreaction of [Cr(tpp)(Cl)(H₂O)] in Toluene.

In the absence of nitrogenous bases, a water molecule present in the toluene solution binds to the chromium ion at the axial coordination site, as in the crystal of [Cr(tpp)(Cl)(H₂O)] (**1**). Figure 4 shows a transient absorption spectrum observed for a toluene solution of **1** at 34 ns after 532 nm laser pulsing at 25.0 °C. The transient spectrum with a positive peak at 435 nm and a negative peak at 450 nm decays according to first-order kinetics with respect to the complex to reproduce the spectrum of the initial complex. Values of k_{obsd} for the decay of the transient spectrum were plotted as a function of the H₂O concentration in toluene in Fig. 5. The slope of the straight line affords the second-order rate constant for the reaction of an H₂O molecule with a transient Cr(III)-tpp complex produced by laser irradi-

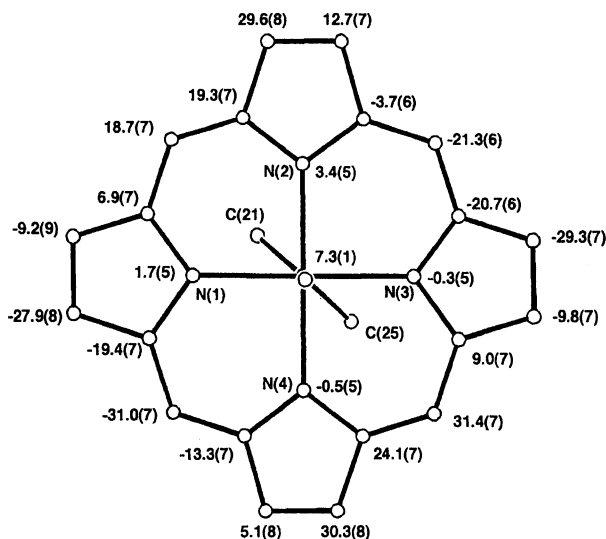


Fig. 3. Diagram of the 24-atom porphyrin core in **2** showing displacements (in unit of 0.01 Å) of each atom from the mean plane of the core. Positive values indicate a displacement on the Cl side of the plane.

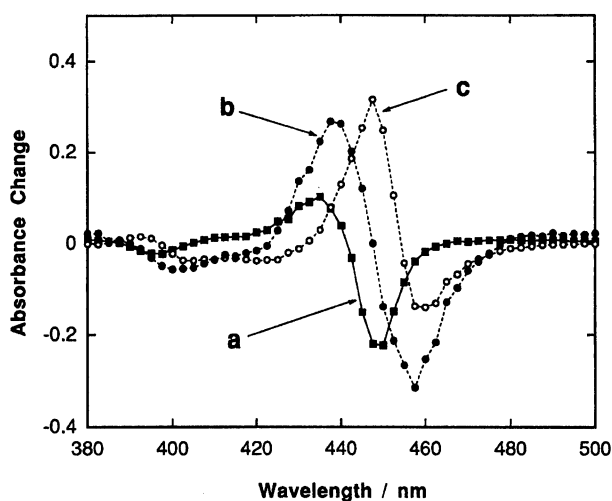
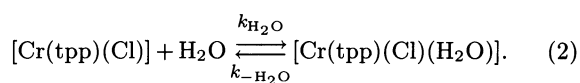


Fig. 4. Transient spectra observed for toluene solutions of the Cr(III)-tpp complex after a 532 nm laser pulse. At 34 ns for $[\text{Cr}(\text{tpp})(\text{Cl})(\text{H}_2\text{O})]$ (a), $C_{\text{Cr-tpp}} = 2.82 \times 10^{-6}$ M, $C_{\text{H}_2\text{O}} = 2.73 \times 10^{-3}$ M. At 34 ns (b) and at 780 ns (c) for $[\text{Cr}(\text{tpp})(\text{Cl})(3\text{-CNpy})]$, $C_{\text{Cr-tpp}} = 8.32 \times 10^{-6}$ M, $C_{3\text{-CNpy}} = 3.15 \times 10^{-3}$ M, $C_{\text{H}_2\text{O}} = 2.99 \times 10^{-3}$ M. $T = 25.0$ °C.

ation. This finding indicates that the transient species can be attributed to $[\text{Cr}(\text{tpp})(\text{Cl})]$, which is produced by photodissociation of the axial H_2O ligand from **1**. Therefore, the decay process of the transient spectrum shown in Fig. 4 is attributed to reaction 2.



Thus, k_{obsd} is given by Eq. 3

$$k_{\text{obsd}} = k_{\text{H}_2\text{O}}[\text{H}_2\text{O}] + k_{-\text{H}_2\text{O}}, \quad (3)$$

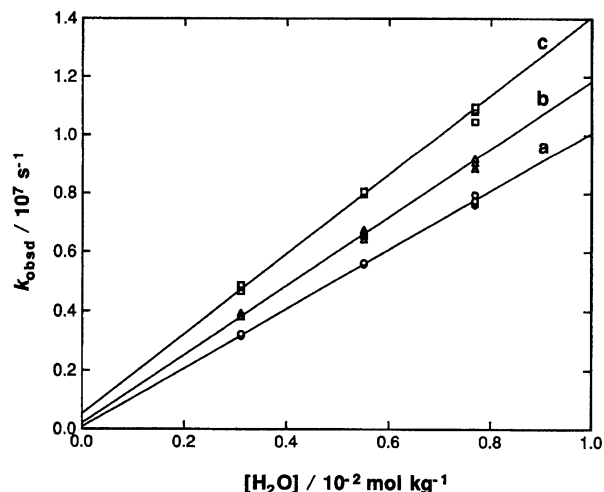


Fig. 5. Dependence of k_{obsd} of the decay of the transient absorption spectrum for $[\text{Cr}(\text{tpp})(\text{Cl})(\text{H}_2\text{O})]$ on the concentration of H_2O . $C_{\text{Cr-tpp}} = (3.11\text{--}3.98) \times 10^{-6}$ mol kg^{-1} . $T = 15.0$ °C (a), 25.0 °C (b), 35.0 °C (c).

where $k_{\text{H}_2\text{O}}$ and $k_{-\text{H}_2\text{O}}$ represent the second-order rate constant for the water recombination reaction and the first-order rate constant for the water dissociation reaction, respectively. Under the present experimental conditions, values of the intercept of the lines in Fig. 5 are relatively small and only the $k_{\text{H}_2\text{O}}$ values were able to be determined accurately: $k_{\text{H}_2\text{O}}/\text{mol}^{-1} \text{ kg s}^{-1} = (1.00 \pm 0.02) \times 10^9$ (15.0 °C), $(1.17 \pm 0.04) \times 10^9$ (25.0 °C), $(1.35 \pm 0.04) \times 10^9$ (35.0 °C). Temperature dependence of $k_{\text{H}_2\text{O}}$ gives $\Delta H_{\text{H}_2\text{O}}^\ddagger = 8.6 \pm 0.4$ kJ mol^{-1} and $\Delta S_{\text{H}_2\text{O}}^\ddagger = -42.4 \pm 1.4$ J $\text{mol}^{-1} \text{ K}^{-1}$.¹⁶⁾ $k_{-\text{H}_2\text{O}}$ values were determined with better accuracy in the laser photolysis of $[\text{Cr}(\text{tpp})(\text{Cl})(3\text{-CNpy})]$ (**3**) as described later.

Photoreaction of $[\text{Cr}(\text{tpp})(\text{Cl})(3\text{-CNpy})]$ in Toluene. Since the photochemical reaction is affected by a small amount of water in toluene, 3-cyanopyridine was used as a nitrogenous base instead of pyridine, which is much more hygroscopic. Reaction curves observed for the laser photolysis of a toluene solution of **3** in the presence of 3-cyanopyridine are shown in Fig. 6. The reaction observed after laser irradiation proceeds with two phases. The first step is completed within 10^{-6} s and the second step has a half-life of ca. 10^{-5} s. Figure 4 shows transient absorption spectra observed at 34 ns and 780 ns after 532 nm laser pulsing for the toluene solution of **3**. As shown in Fig. 6, the absorbance change at 34 ns after laser irradiation does not depend on $[\text{H}_2\text{O}]$ or $[3\text{-CNpy}]$, while the absorbance change observed at 780 ns after the laser pulse is a function of $[\text{H}_2\text{O}]$ and $[3\text{-CNpy}]$. Since the second transient spectrum is identical with the difference spectrum obtained by subtracting the spectrum of **3** from that of **1**, the second transient should be attributed to $[\text{Cr}(\text{tpp})(\text{Cl})(\text{H}_2\text{O})]$ (**1**). On the other hand, the first transient spectrum has a positive peak at 437.5 nm and a neg-

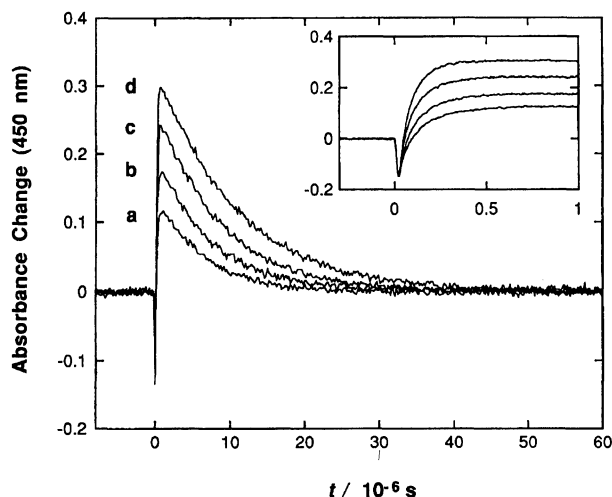


Fig. 6. Reaction curves for laser photolysis of the toluene solution of $[\text{Cr}(\text{tpp})(\text{Cl})(3\text{-CNpy})]$ in the presence of various amounts of water at 25.0°C . The inset shows the reaction curves at the beginning of the reaction. Energy of the laser pulse at 532 nm for each run was kept constant. $C_{\text{Cr-tpp}} = 9.00 \times 10^{-6}\text{ mol kg}^{-1}$, $C_{3\text{-CNpy}} = 9.30 \times 10^{-3}\text{ mol kg}^{-1}$, $C_{\text{H}_2\text{O}}/\text{mol kg}^{-1} = 1.97 \times 10^{-3}$ (a), 2.90×10^{-3} (b), 4.57×10^{-3} (c), 6.61×10^{-3} (d).

ative peak at 457.5 nm . The first transient, therefore, seems to be the same as the transient species observed after laser irradiation of **1**, i.e., the five-coordinate intermediate $[\text{Cr}(\text{tpp})(\text{Cl})]$.

Yields of the intermediate $[\text{Cr}(\text{tpp})(\text{Cl})]$ from **1** and **3** caused by the laser irradiation, $R_{\text{H}_2\text{O}}$ and R_{CNpy} , respectively, are defined as

$$R_{\text{H}_2\text{O}} = \Delta A(\mathbf{1}) C_{\text{Cr-tpp}}(\mathbf{1})^{-1} (\varepsilon(\text{int}) - \varepsilon(\mathbf{1}))^{-1}, \quad (4)$$

$$R_{\text{CNpy}} = \Delta A(\mathbf{3}) C_{\text{Cr-tpp}}(\mathbf{3})^{-1} (\varepsilon(\text{int}) - \varepsilon(\mathbf{3}))^{-1}, \quad (5)$$

where $\varepsilon(\mathbf{1})$, $\varepsilon(\mathbf{3})$, and $\varepsilon(\text{int})$ represent the molar absorption coefficients of **1**, **3**, and $[\text{Cr}(\text{tpp})(\text{Cl})]$, respectively, and $\Delta A(\mathbf{1})$ and $\Delta A(\mathbf{3})$ denote the absorbance changes observed just after laser irradiation of the solutions of **1** and **3**, respectively, at a given wavelength. $C_{\text{Cr-tpp}}(\mathbf{1})$ and $C_{\text{Cr-tpp}}(\mathbf{3})$ are total concentrations of the complex in the solutions of **1** and **3**, respectively. Since $\varepsilon(\text{int})$ in Eqs. 4 and 5 is identical, we have

$$R_{\text{H}_2\text{O}}^{-1} = (\varepsilon(\mathbf{3}) - \varepsilon(\mathbf{1})) \Delta A(\mathbf{1})^{-1} C_{\text{Cr-tpp}}(\mathbf{1}) + R_{\text{CNpy}}^{-1} \Delta A(\mathbf{1})^{-1} C_{\text{Cr-tpp}}(\mathbf{1}) \Delta A(\mathbf{3}) C_{\text{Cr-tpp}}(\mathbf{3})^{-1}. \quad (6)$$

Values of $\varepsilon(\mathbf{1})$, $\varepsilon(\mathbf{3})$, $\Delta A(\mathbf{1})$, and $\Delta A(\mathbf{3})$ were determined experimentally at every 2.5 nm over the range between 380 and 500 nm . Since $R_{\text{H}_2\text{O}}$ and R_{CNpy} are independent of the wavelength, these values were determined so as to satisfy simultaneously the equations defined by Eq. 6 for each wavelength: $R_{\text{H}_2\text{O}} = 0.54 \pm 0.01$, $R_{\text{CNpy}} = 0.39 \pm 0.01$. The determined spectrum of $[\text{Cr}(\text{tpp})(\text{Cl})]$ is shown in Fig. 7.

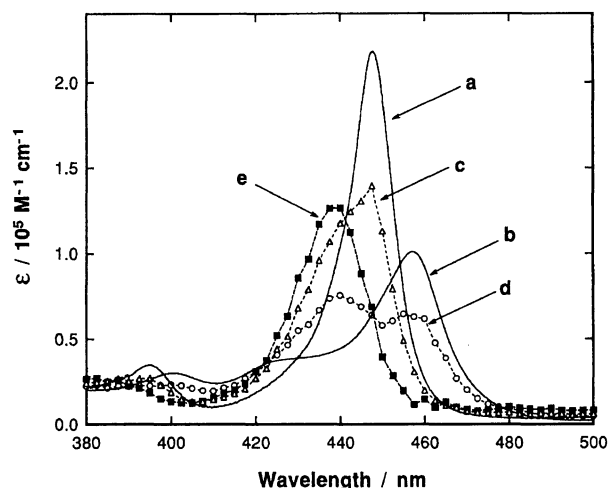
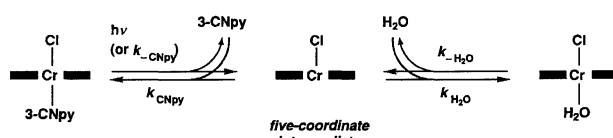
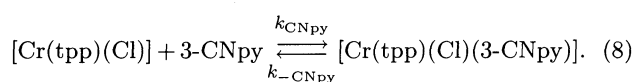
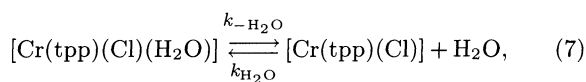


Fig. 7. Visible absorption spectra of **1** (a) and **3** (b), transient absorption spectra of **1** (c) and **3** (d) at 34 ns after a laser pulse, and calculated absorption spectrum of the five-coordinate intermediate $[\text{Cr}(\text{tpp})(\text{Cl})]$ (e). Conditions are the same as shown in Fig. 4.

The first step of the reaction observed after laser irradiation shown in Fig. 6 is attributed to the reaction of the photoinduced five-coordinate intermediate $[\text{Cr}(\text{tpp})(\text{Cl})]$ with H_2O or 3-CNpy in the bulk solution, leading to **1** and **3**, respectively. Produced **1** is also a transient species with respect to the axial substitution in the presence of 3-CNpy . Thus the coordinated water molecule is easily substituted by a 3-CNpy molecule to give the initial complex **3**, which is the reaction attributable to the second step of the reaction. According to these findings, the reactions induced by laser irradiation of the toluene solution of **3** are shown in Scheme 1.

Rates of the second step for the reaction system of **3** were measured under various conditions, where H_2O and 3-CNpy are present in a large excess over the $\text{Cr}(\text{III})\text{-tpp}$ complex. The reaction is first order with respect to **1**. At a constant concentration of H_2O in the bulk, k_{obsd} increases with an increase of $[3\text{-CNpy}]$ and approaches a limited value at higher concentrations of 3-CNpy , while it decreases with an increase of $[\text{H}_2\text{O}]$ in the bulk at a constant 3-CNpy concentration, as shown in Fig. 8. These features can be interpreted by a dissociative mechanism indicated by Eqs. 7 and 8.



Scheme 1.

The value of k_{CNpy} was previously determined to be $3.1 \times 10^2 \text{ s}^{-1}$ at 25.0°C .^{2b)} Since k_{CNpy} contributes little to k_{obsd} under the present experimental conditions, Eq. 9 is obtained by applying the steady-state approximation to the five-coordinate intermediate $[\text{Cr}(\text{tpp})(\text{Cl})]$.

$$k_{\text{obsd}} = k_{-\text{H}_2\text{O}}([3\text{-CNpy}]/[\text{H}_2\text{O}])(k_{\text{H}_2\text{O}}/k_{\text{CNpy}} + [3\text{-CNpy}]/[\text{H}_2\text{O}])^{-1}. \quad (9)$$

Values of $k_{-\text{H}_2\text{O}}$ and $k_{\text{H}_2\text{O}}/k_{\text{CNpy}}$ at each temperature were determined by fitting k_{obsd} obtained at various concentrations of H_2O and 3-CNpy to Eq. 9 by use of a least-squares program, and are listed in Table 4. Eyring's plots of $k_{-\text{H}_2\text{O}}$ and $k_{\text{H}_2\text{O}}/k_{\text{CNpy}}$ proved linear within the experimental errors. Therefore, the enthalpy and entropy of activation were de-

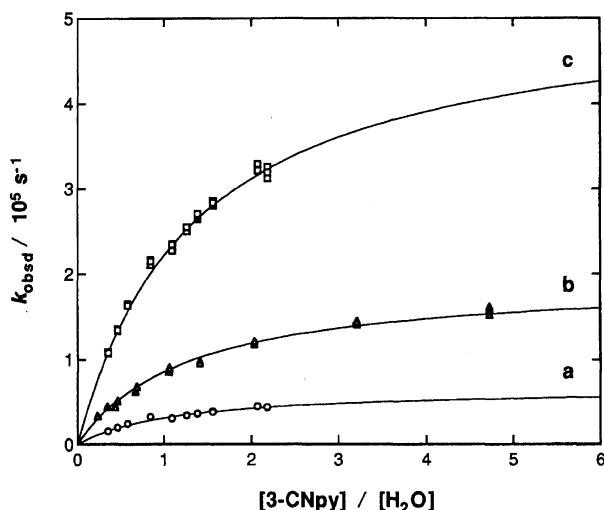


Fig. 8. Plots of k_{obsd} for the second decay process of the laser photolysis of $[\text{Cr}(\text{tpp})(\text{Cl})-(3\text{-CNpy})]$ solution as a function of the ratio of the concentrations of the ligands, $[3\text{-CNpy}]/[\text{H}_2\text{O}]$. $C_{\text{Cr-tpp}} = (0.55\text{--}1.78) \times 10^{-5} \text{ mol kg}^{-1}$, $C_{3\text{-CNpy}} = (2.44\text{--}9.30) \times 10^{-3} \text{ mol kg}^{-1}$, $C_{\text{H}_2\text{O}} = (1.97\text{--}11.1) \times 10^{-3} \text{ mol kg}^{-1}$. $T = 15.0^\circ\text{C}$ (a), 25.0°C (b), 35.0°C (c).

Table 4. Rate Constants and Activation Parameters^{a)} for the Water Substitution Reaction of $[\text{Cr}(\text{tpp})(\text{Cl})(\text{H}_2\text{O})]$ by 3-CNpy in Toluene

| $T/^\circ\text{C}$ | $k_{-\text{H}_2\text{O}}/\text{s}^{-1}$ | $k_{\text{H}_2\text{O}}/k_{\text{CNpy}}$ |
|--|---|--|
| 15.0 | $(6.68 \pm 0.20) \times 10^4$ | 1.12 ± 0.06 |
| 25.0 | $(1.95 \pm 0.05) \times 10^5$ | 1.29 ± 0.05 |
| 35.0 | $(5.18 \pm 0.08) \times 10^5$ | 1.30 ± 0.03 |
| $\Delta H_{-\text{H}_2\text{O}}^\ddagger$ | | |
| 73.0 ± 1.5 | | |
| $\Delta S_{-\text{H}_2\text{O}}^\ddagger$ | | |
| 101.0 ± 5.1 | | |
| $\Delta H_{\text{H}_2\text{O}}^\ddagger - \Delta H_{\text{CNpy}}^\ddagger$ | | |
| 5.2 ± 2.7 | | |
| $\Delta S_{\text{H}_2\text{O}}^\ddagger - \Delta S_{\text{CNpy}}^\ddagger$ | | |
| 19.2 ± 9.1 | | |

a) $\Delta H^\ddagger/\text{kJ mol}^{-1}$, $\Delta S^\ddagger/\text{J mol}^{-1} \text{ K}^{-1}$

termined by simultaneously fitting the variable-temperature data to Eq. 9 and the Eyring equation ($k = (k_B T/h) \exp(-\Delta H^\ddagger/(RT) + \Delta S^\ddagger/R)$), and are summarized in Table 4. k_{CNpy} values and corresponding activation parameters can be evaluated by using the kinetic parameters for $k_{\text{H}_2\text{O}}/k_{\text{CNpy}}$ and those for $k_{\text{H}_2\text{O}}$ determined for the reaction system of **1**: $k_{\text{CNpy}} = 9.2 \times 10^8 \text{ mol}^{-1} \text{ kg s}^{-1}$ (25.0°C), $\Delta H^\ddagger = 3.4 \pm 2.7 \text{ kJ mol}^{-1}$, and $\Delta S^\ddagger = -62 \pm 9 \text{ J mol}^{-1} \text{ K}^{-1}$.

The first step for the reaction system of **3**, which is the reaction of the five-coordinate complex $[\text{Cr}(\text{tpp})(\text{Cl})]$ with H_2O and 3-CNpy to lead to **1** and **3**, respectively, was also first-order with respect to the complex. k_{obsd} increases linearly with the increase of $[\text{H}_2\text{O}]$ and $[3\text{-CNpy}]$. k_{obsd} is, thus, expressed as

$$k_{\text{obsd}} = k_{\text{H}_2\text{O}}[\text{H}_2\text{O}] + k_{-\text{H}_2\text{O}} + k_{\text{CNpy}}[3\text{-CNpy}] + k_{-\text{CNpy}}. \quad (10)$$

Values of $(k_{\text{obsd}} - k_{-\text{H}_2\text{O}} - k_{-\text{CNpy}})[3\text{-CNpy}]^{-1}$ are plotted against $[\text{H}_2\text{O}][3\text{-CNpy}]^{-1}$ in Fig. 9. By least-squares fitting, $k_{\text{H}_2\text{O}}$ and k_{CNpy} were obtained: $k_{\text{H}_2\text{O}} = (1.18 \pm 0.03) \times 10^9 \text{ mol}^{-1} \text{ kg s}^{-1}$, $k_{\text{CNpy}} = (9.1 \pm 0.4) \times 10^8 \text{ mol}^{-1} \text{ kg s}^{-1}$ ($T = 25.0^\circ\text{C}$). The value of $k_{\text{H}_2\text{O}}$ is in excellent agreement with that determined in the $[\text{Cr}(\text{tpp})(\text{Cl})(\text{H}_2\text{O})]$ system (vide supra). Moreover, the ratio $k_{\text{H}_2\text{O}}/k_{\text{CNpy}} = 1.29 \pm 0.06$ is the same as that (1.29 ± 0.05) determined for the axial substitution reaction of **1** by 3-CNpy, as listed in Table 4. This agreement implies that the five-coordinate intermediate $[\text{Cr}(\text{tpp})(\text{Cl})]$ generated by laser irradiation should be the same as the species which is assumed to be an intermediate for the axial water substitution of **1** by 3-CNpy.

Quantum Yield of Photodissociation of Axial

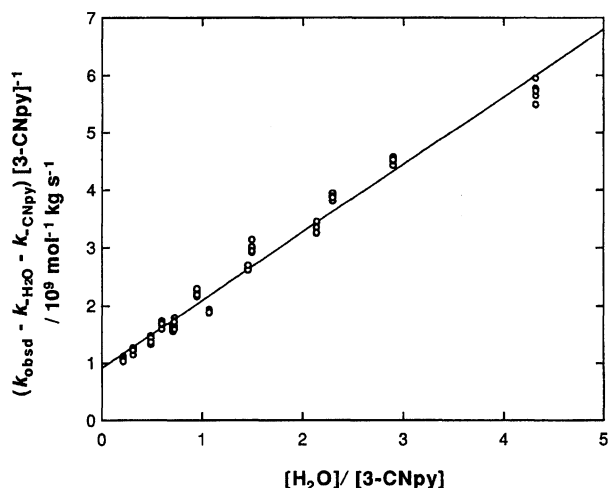
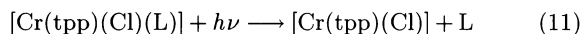


Fig. 9. Relationship between the pseudo-first-order rate constant k_{obsd} of the first decay process of the laser photolysis of the $[\text{Cr}(\text{tpp})(\text{Cl})-(3\text{-CNpy})]$ solution and the ratio of the concentrations of the ligands, $[\text{H}_2\text{O}]/[3\text{-CNpy}]$, in the bulk at $T = 25.0^\circ\text{C}$. $C_{\text{Cr-tpp}} = (0.55\text{--}1.78) \times 10^{-5} \text{ mol kg}^{-1}$, $C_{3\text{-CNpy}} = (2.44\text{--}9.30) \times 10^{-3} \text{ mol kg}^{-1}$, $C_{\text{H}_2\text{O}} = (1.97\text{--}11.1) \times 10^{-3} \text{ mol kg}^{-1}$.

Ligand. Quantum yield of the photodissociation of the axial ligand L from [Cr(tpp)(Cl)(L)] (Eq. 11) was



measured. The number of photons absorbed by [Cr(tpp)(Cl)(L)], I_{abs} , at a laser excitation wavelength was determined by measuring the triplet-triplet absorption of [Zn(tpp)] in a benzene solution that has the same absorbance as that of the toluene solution of [Cr(tpp)(Cl)(L)] at the laser excitation wavelength. The initial absorbance change, ΔA_{T} , of the triplet [Zn(tpp)] at 470 nm after a laser pulsing is expressed as

$$\Delta A_{\text{T}} = \phi_{\text{T}} \Delta \varepsilon_{470} I_{\text{abs}}, \quad (12)$$

where ϕ_{T} and $\Delta \varepsilon_{470}$ represent the triplet yield of [Zn(tpp)] and the difference of the molar absorption coefficient of the triplet [Zn(tpp)] and of its ground state at 470 nm: $\phi_{\text{T}} = 0.83$, $\Delta \varepsilon_{470} = 7.3 \times 10^4 \text{ M}^{-1} \text{ cm}^{-1}$.¹⁷⁾ The quantum yield, ϕ_{dis} , for the photodissociation of L from [Cr(tpp)(Cl)(L)] is expressed as

$$\phi_{\text{dis}} = \Delta A_{\text{dis}} \Delta \varepsilon^{-1} I_{\text{abs}}^{-1}, \quad (13)$$

where ΔA_{dis} and $\Delta \varepsilon$ are the absorbance change at a monitoring wavelength just after laser excitation and the difference in the molar absorption coefficient between [Cr(tpp)(Cl)] and [Cr(tpp)(Cl)(L)] at the wavelength, respectively. Thus, we have Eq. 14:

$$\phi_{\text{dis}} = \Delta A_{\text{dis}} \Delta A_{\text{T}}^{-1} \Delta \varepsilon_{470} \Delta \varepsilon^{-1} \phi_{\text{T}}. \quad (14)$$

Determined ϕ_{dis} values listed in Table 5 are not dependent on the excitation wavelength, as in the case of the photochemistry of [Cr(tpp)(Cl)(py)] in acetone.⁷⁾

In order to test the effect of dioxygen dissolved in toluene on the quantum yield, laser photolysis experiments was conducted for both the degassed and air-saturated solutions. It has been confirmed that dioxygen has no effect on the quantum yield of photodissociation of the axial ligand in the present reaction systems.

Discussion

There have not been many reports on the molecular structures of Cr(II), Cr(III), Cr(IV), and Cr(V) porphyrin complexes.^{18,19)} For Cr(III) porphyrins, only two reports are available, i.e., [Cr(tpp)(N₃)(py)] and [Cr(tpp)(OC₆H₅)(tetrahydrofuran)].¹⁹⁾ The interatomic distances between Cr and N atoms of pyridine positioned in trans of chloride and azide are close to each other, i.e., 2.140(5) Å for [Cr(tpp)(Cl)(py)](**2**) and 2.135(4) Å for [Cr(tpp)(N₃)(py)],^{19a)} reflecting the similar trans influence for the axial Cl⁻ and N₃⁻ ligands. The equatorial Cr-N distances of 2.031(2) Å of **1** and 2.016(6)–2.037(5) Å of **2** are similar to those found in [Cr(tpp)(N₃)(py)] (2.023(4)–2.031(5) Å)^{19a)} and in [Cr(tpp)(OC₆H₅)(tetrahydrofuran)] (2.035(5), 2.038(7) Å).^{19b)}

The Cr-Cl distances vary with their trans ligands, i.e., the Cr-Cl distance in **1** (2.242(3) Å) is significantly shorter than that in **2** (2.311(2) Å). The shorter Cr-Cl distance in **1** can be attributed to the weaker bonding for Cr-O(H₂O) (2.239(3) Å) in the trans position, compared to Cr-N(5) (2.140(5) Å) for **2**. This is well described by comparison with the results for the same type of Co(III) porphyrins. The Co-O(H₂O) distance (1.979(3) Å) in [Co^{III}(tpp)(Cl)(H₂O)]²⁰⁾ is comparable to the Co-N(py) distance (1.978(8) Å) in [Co^{III}(tpp)(Cl)(py)],²¹⁾ and consequently, the difference in the Co-Cl distance (2.216(1) Å for the former and 2.251(3) Å for the latter) is considerably smaller than that for Cr(III) complexes **1** and **2**. Furthermore, the weaker bond energy of Cr-O(H₂O) for **1** in comparison with that of Cr-N(py) for **2** was demonstrated by the difference in the rate constants of the axial ligand dissociation determined in toluene, i.e., $k_{-\text{H}_2\text{O}} = 1.95 \times 10^5 \text{ s}^{-1}$ (vide infra) and $k_{-\text{py}} = 8.24 \text{ s}^{-1}$.^{2b)}

Photophysical and photochemical properties of the Cr(III) porphyrin complex have been investigated to elucidate the dynamics of the excited states of the complex in solution.²²⁾ Excitation of the complex usually leads to the generation of the porphyrin ($\pi\pi^*$) excited singlet state ⁴S₁ and triplet states ⁴T₁ and ⁶T₁. Since the Cr(III) porphyrin complex is paramagnetic, it shows little normal ($\pi\pi^*$) fluorescence. The fluorescence quantum yield in ethanol was determined to be less than 10⁻⁴, and the rate constant of non-radiative decay from the first excited singlet state was evaluated to be larger than $2 \times 10^{11} \text{ s}^{-1}$. Triplet state fluorescence from tripquartet and tripsextet states was observed in ethanol, but its intensity was extremely weak. These findings were interpreted as due to the influence of the paramagnetic Cr(III) ion on the rate of the deactivation of the excited states, where the rates of non-radiative processes are much faster than those for the diamagnetic metalloporphyrins. In the present study, the six-coordinate complexes [Cr(tpp)(Cl)(L)] (L=H₂O, 3-CNpy) have been used for laser photolysis. Here, the axial ligand dissociation is promoted by laser irradiation besides other possible photophysical processes. The quantum yield ϕ_{dis} of the photodissociation of the axial ligand L from [Cr(tpp)(Cl)(L)] in toluene is large for the present systems (see Table 5). Although it is expected that the excited triplet state would show the transient absorption spectrum around 470 nm, which was demonstrated for [Cr(tpp)(Cl)(py)] and [Cr(tpp)(Cl)(acetone)] in the acetone solution,⁷⁾ such an excited triplet state was not clearly observed in the toluene solution. Therefore, high ϕ_{dis} values and the extremely low yield of the triplet state indicate that the axial ligand dissociation due to laser irradiation should occur at the excited singlet state ⁴S₁ with a very high efficiency in toluene.

The five-coordinate complex [Cr(tpp)(Cl)] generated by laser irradiation is considered to be in its electronic

Table 5. Values of Quantum Yield for Photodissociation of the Axial Ligand L from [Cr(tpp)(Cl)(L)] in Toluene upon Laser Irradiation at 532 and 355 nm

| Complex | Irradiation wavelength/nm | ϕ_{dis} |
|-------------------------------------|---------------------------|---------------------|
| [Cr(tpp)(Cl)(H ₂ O)] (1) | 532 | 0.94±0.06 |
| | 355 | 0.92±0.06 |
| [Cr(tpp)(Cl)(3-CNpy)] (3) | 532 | 0.72±0.05 |
| | 355 | 0.77±0.05 |

Table 6. Kinetic Parameters for Reaction of Five-Coordinate Intermediate [Cr(tpp)(Cl)] with Water and Nitrogenous Bases L

| L | $B^{\text{a)}}$ | $k_{\text{L}}/\text{mol}^{-1}\text{kg s}^{-1}$ ^{b)} | $\Delta H_{\text{L}}^{\ddagger}/\text{kJ mol}^{-1}$ | $\Delta S_{\text{L}}^{\ddagger}/\text{J mol}^{-1}\text{K}^{-1}$ |
|------------------------|-----------------|--|---|---|
| H ₂ O | 665 | 1.17×10^9 ^{c)} | 8.6 ± 0.4 ^{c)} | -42.4 ± 1.4 ^{c)} |
| 3-CNpy | 843 | 9.2×10^8 ^{c)} | 3.4 ± 2.7 | -62 ± 9 |
| 4-CNpy | 851 | 9.9×10^8 | 2.8 ± 3.3 | -63 ± 11 |
| 3-Clpy | 866 | 9.5×10^8 | 5.7 ± 3.4 | -54 ± 12 |
| 3-Acpy | 876 | 8.5×10^8 | 3.7 ± 3.3 | -61 ± 11 |
| 4-Acpy | 877 | 9.8×10^8 | 3.4 ± 3.3 | -61 ± 11 |
| py | 892 | 8.1×10^8 | 3.1 ± 3.3 | -64 ± 11 |
| 3-Mepy | 905 | 7.5×10^8 | 3.5 ± 3.5 | -63 ± 12 |
| 4-Mepy | 909 | 8.9×10^8 | 3.0 ± 3.4 | -63 ± 11 |
| 3,5-Me ₂ py | 911 | 7.1×10^8 | 3.6 ± 3.2 | -63 ± 11 |
| 1-Meim | 925 | 8.6×10^8 | 4.7 ± 3.1 | -58 ± 11 |

a) Gas phase basicity in kJ mol^{-1} (Ref. 23). b) At 25.0 °C. c) Determined directly, while estimated in the other cases (see in text).

ground state, judging from the photophysical and photochemical properties of the Cr(III) porphyrin complex mentioned above. Further evidence is the consistency of the rate constant ratio of $k_{\text{H}_2\text{O}}/k_{\text{CNpy}}$ determined by two independent experiments, i.e., one is the reaction observed for the photogenerated [Cr(tpp)(Cl)] and the other is the axial substitution reaction of [Cr(tpp)(Cl)(H₂O)] by 3-CNpy (the second process of the 3-CNpy system) which is a pure thermal reaction. [Cr(tpp)(Cl)] is the complex proposed as a reactive intermediate for the axial substitution reaction of the six-coordinate [Cr(tpp)(Cl)(L)].^{1f,2)} We have reported the kinetics of the substitution reaction of the axial ligand L in [Cr(tpp)(Cl)(L)] by 1-methylimidazole (1-Meim) in toluene as studied by a stopped-flow technique, where L represents pyridine or various β - and γ -substituted pyridines.^{2b)} The rate law of the reaction is quite similar to Eq. 9, where H₂O and 3-CNpy are substituted by L and 1-Meim, respectively. Although the basicity values of these substituted pyridines are different, the values of $k_{\text{L}}/k_{1\text{-Meim}}$ are similar and fall into a very narrow range around unity. The very low discriminating ability of [Cr(tpp)(Cl)] toward these substituted pyridines indicates the extremely high reactivity of this intermediate. In the present work, the rate constant k_{L} (L=3-CNpy) was directly determined to be $9.2 \times 10^8 \text{ mol}^{-1} \text{ kg s}^{-1}$ at 25.0 °C. By using the values of the ratio $k_{\text{L}}/k_{1\text{-Meim}}$ previously determined for various substituted pyridines and the rate constant k_{L} determined in the present study for L=3-CNpy, k_{L} and corresponding activation parameters for other substituted pyridines can be es-

timated as listed in Table 6. The recombination rate constant k_{L} is large (ca. $10^9 \text{ mol}^{-1} \text{ kg s}^{-1}$) for all L. The activation enthalpy $\Delta H_{\text{L}}^{\ddagger}$ is small for each case and changes little with the ligand basicity. These findings strongly indicate that the diffusion-controlled process should be rate-determining for the recombination reaction between [Cr(tpp)(Cl)] and L. A rate constant for the diffusion-controlled process of a bimolecular reaction is given by $k=4\pi(D_{\text{A}}+D_{\text{B}})r_{\text{c}}$,²⁴⁾ where D_{A} and D_{B} represent the self-diffusion coefficient of molecules A and B, respectively, and r_{c} is the hard-sphere collision distance. The self-diffusion coefficient is given by the Stokes law: $D=k_{\text{B}}T/(6\pi\eta r)$, where η is a viscosity of the solvent. Assumption of $r_{\text{c}}=r_{\text{A}}+r_{\text{B}}$ leads to Eq. 15:

$$k = (2k_{\text{B}}T/(3\eta))(r_{\text{A}} + r_{\text{B}})^2/(r_{\text{A}}r_{\text{B}}). \quad (15)$$

Temperature dependence of the viscosity is empirically given by Andrade's equation: $\ln \eta = A + E/(RT)$. Here, E corresponds to the activation energy of the rate process of the viscous flow in the medium. Therefore, the rate constant k is given by

$$k = (2k_{\text{B}}T/(3\exp A)) \{(r_{\text{A}} + r_{\text{B}})^2/(r_{\text{A}}r_{\text{B}})\} \exp(-E/(RT)). \quad (16)$$

The temperature dependence of the viscosity of toluene gives $E=8.8 \text{ kJ mol}^{-1}$,²⁵⁾ which is close to the activation energy of $k_{\text{H}_2\text{O}}$. The coincidence of these values is evidence for the diffusion-controlled process. However, the $k_{\text{H}_2\text{O}}$ value is by one order of magnitude smaller than the rate constant evaluated from Eq. 16, which value

is in the order of $10^{10} \text{ mol}^{-1} \text{ kg s}^{-1}$. The difference between the two values may be due to the geometrical factor that governs the recombination reaction between $[\text{Cr}(\text{tpp})(\text{Cl})]$ and H_2O . The reaction occurs effectively only when the water molecule approaches the complex from its vacant coordination site.

This work was supported by Grants-in-Aid for Scientific Research in a Priority Area (Nos. 04215213 and 06239267) and for Scientific Research (Nos. 04403011 and 06640779) from the Ministry of Education, Science and Culture.

References

- 1) a) E. B. Fleischer and M. Krishnamurthy, *J. Am. Chem. Soc.*, **93**, 3784 (1971); b) E. B. Fleischer and M. Krishnamurthy, *J. Coord. Chem.*, **2**, 89 (1972); c) M. Krishnamurthy, *Inorg. Chim. Acta*, **26**, 137 (1978); d) K. R. Ashley, J. G. Leipoldt, and V. K. Joshi, *Inorg. Chem.*, **19**, 1608 (1980); e) J. G. Leipoldt, S. S. Basson, and D. R. Rabie, *J. Inorg. Nucl. Chem.*, **43**, 3239 (1981); f) P. O'Brien and D. A. Sweigart, *Inorg. Chem.*, **21**, 2094 (1982); g) J. G. Leipoldt, R. van Eldik, and H. Kelm, *Inorg. Chem.*, **22**, 4146 (1983); h) J. G. Leipoldt and H. Meyer, *Polyhedron*, **6**, 1361 (1987); i) K. R. Ashley and J. Kuo, *Inorg. Chem.*, **27**, 3556 (1988); j) K. R. Ashley and I. Trent, *Inorg. Chim. Acta*, **163**, 159 (1989).
- 2) a) M. Inamo, T. Sumi, N. Nakagawa, S. Funahashi, and M. Tanaka, *Inorg. Chem.*, **28**, 2688 (1989); b) M. Inamo, S. Sugiura, H. Fukuyama, and S. Funahashi, *Bull. Chem. Soc. Jpn.*, **67**, 1848 (1994).
- 3) a) E. B. Fleischer, S. Jacobs, and L. Mestichelli, *J. Am. Chem. Soc.*, **90**, 2527 (1968); b) R. F. Pasternack and M. A. Cobb, *Biochem. Biophys. Res. Commun.*, **51**, 507 (1973); c) E. B. Fleischer and M. Krishnamurthy, *Ann. N. Y. Acad. Sci.*, **206**, 32 (1973); d) R. F. Pasternack and M. A. Cobb, *J. Inorg. Nucl. Chem.*, **35**, 4327 (1973); e) K. R. Ashley, M. Berggren, and M. Cheng, *J. Am. Chem. Soc.*, **97**, 1422 (1975); f) R. F. Pasternack, M. A. Cobb, and N. Sutin, *Inorg. Chem.*, **14**, 866 (1975); g) K. R. Ashley and S. Au-Young, *Inorg. Chem.*, **15**, 1937 (1976); h) R. F. Pasternack and G. R. Parr, *Inorg. Chem.*, **15**, 3087 (1976); i) K. R. Ashley, *J. Inorg. Nucl. Chem.*, **39**, 357 (1976); j) K. R. Ashley and J. G. Leipoldt, *Inorg. Chem.*, **20**, 2326 (1981); k) J. G. Leipoldt, S. S. Basson, G. J. Lamprecht, and R. D. Rabie, *Inorg. Chim. Acta*, **51**, 67 (1981); l) S. Funahashi, M. Inamo, K. Ishihara, and M. Tanaka, *Inorg. Chem.*, **21**, 447 (1982); m) A. Mahmood, H. Liu, J. G. Jones, J. O. Edwards, and D. A. Sweigart, *Inorg. Chem.*, **27**, 2149 (1988).
- 4) a) M. Krishnamurthy, *Inorg. Chim. Acta*, **25**, 215 (1977); b) K. R. Ashley, S. Shyu, and J. G. Leipoldt, *Inorg. Chem.*, **19**, 1613 (1980).
- 5) a) D. Lavalette, C. Tetreau, and M. Momenteau, *J. Am. Chem. Soc.*, **101**, 5395 (1979); b) M. Hoshino, *Chem. Phys. Lett.*, **120**, 50 (1985); c) M. Hoshino and M. Kogure, *J. Phys. Chem.*, **93**, 5478 (1989); d) M. Hoshino, K. Ueda, M. Takahashi, M. Yamaji, Y. Hama, and Y. Miyazaki, *J. Phys. Chem.*, **96**, 8863 (1992); e) M. Hoshino, K. Ozawa, H. Seki, and P. C. Ford, *J. Am. Chem. Soc.*, **115**, 9568 (1993).
- 6) a) C. Tetreau, D. Lavalette, and M. Momenteau, *J. Am. Chem. Soc.*, **105**, 1506 (1983); b) C. D. Tait, D. Holten, and M. Gouterman, *J. Am. Chem. Soc.*, **106**, 6653 (1984); c) M. Hoshino, S. Arai, M. Yamaji, and Y. Hama, *J. Phys. Chem.*, **90**, 2109 (1986); d) M. Hoshino, M. Kogure, K. Amano, and T. Hinohara, *J. Phys. Chem.*, **93**, 6655 (1989).
- 7) a) M. Yamaji, Y. Hama, and M. Hoshino, *Chem. Phys. Lett.*, **165**, 309 (1990); b) M. Yamaji, *Inorg. Chem.*, **30**, 2949 (1991).
- 8) M. Hoshino and Y. Kashiwagi, *J. Phys. Chem.*, **94**, 673 (1990).
- 9) D. A. Summerville, R. D. Jones, B. M. Hoffman, and F. Basolo, *J. Am. Chem. Soc.*, **99**, 8195 (1977).
- 10) P. Main, S. E. Hull, L. Lessinger, G. Germain, J.-P. Declercq, and M. M. Woolfson, "MULTAN 78: A System of Computer Programs for the Automatic Solution of Crystal Structures from X-Ray Diffraction Data," Univ. of York, England and Louvain, Belgium (1978).
- 11) G. M. Sheldrick, "SHELXS-86, Program for Crystal Structure Determination," University of Göttingen, Germany (1986).
- 12) "Programs of Structure Determination Package," MAC Science, Yokohama (1992).
- 13) T. Sakurai and K. Kobayashi, *Rigaku Kenkyusho Hokoku*, **55**, 69 (1979).
- 14) "International Tables for X-Ray Crystallography," Kynoch, Birmingham, England (1974), Vol. IV.
- 15) a) J. L. Hoard, in "Porphyrins and Metalloporphyrins," ed by K. M. Smith, Elsevier, Amsterdam (1975), pp. 317–380; b) W. R. Scheidt, in "The Porphyrins," ed by D. Dolphin, Academic Press, New York (1978), Vol. 3, pp. 463–511.
- 16) Errors of the kinetic parameters are standard deviations determined from the least-squares fit of the data.
- 17) J. K. Hurley, N. Sinai, and H. Linschitz, *Photochem. Photobiol.*, **38**, 9 (1983).
- 18) a) J. T. Groves, W. J. Kruper, Jr., R. C. Haushalter, and W. M. Butler, *Inorg. Chem.*, **21**, 1363 (1982); b) J. T. Groves, T. Takahashi, and W. M. Butler, *Inorg. Chem.*, **22**, 884 (1983); c) W. R. Scheidt, A. C. Brinegar, J. F. Kirner, and C. A. Reed, *Inorg. Chem.*, **18**, 3610 (1976); d) W. R. Scheidt and C. A. Reed, *Inorg. Chem.*, **17**, 710 (1978); e) J. R. Budge, B. M. K. Gatehouse, M. C. Nesbit, and B. O. West, *J. Chem. Soc., Chem. Commun.*, **1981**, 370; f) J. T. Groves, R. Quinn, T. J. McMurphy, M. Nakamura, G. Lang, and B. Boso, *J. Am. Chem. Soc.*, **107**, 354 (1985); g) D. J. Liston, B. J. Kennedy, K. S. Murray, and B. O. West, *Inorg. Chem.*, **24**, 1561 (1985).
- 19) a) S. Huoming, G. Shuzhen, L. Yongsheng, and J. Rizhen, *Chin. J. Appl. Chem.*, **8**, 67 (1991); b) A. L. Balch, L. Latos-Grazynski, B. C. Noll, M. M. Olmstead, and E. P. Zovinka, *Inorg. Chem.*, **31**, 1148 (1992).
- 20) Y. Iimura, T. Sakurai, and K. Yamamoto, *Bull. Chem. Soc. Jpn.*, **61**, 821 (1988).
- 21) T. Sakurai, K. Yamamoto, N. Seino, and M. Katsuta, *Acta Crystallogr., Sect. B*, **31**, 2514 (1975).
- 22) a) M. Gouterman, L. K. Hanson, G.-E. Khalil, W. R. Leenstra, and J. W. Buchler, *J. Chem. Phys.*, **62**, 2343 (1975); b) A. Harriman, *J. Chem. Soc., Faraday Trans. 1*, **78**, 2727 (1982).
- 23) The gas phase basicity of a molecule is defined in terms of the hypothetical reaction (Eq. 17):



The gas phase basicity, B , is the negative of the energy change associated with this reaction. These values are cited in *Journal of Physical and Chemical Reference Data*, Volume 13, The American Chemical Society and the American

Institute of Physics for the National Bureau of Standards (1984).

24) M. V. Smoluchowski, *Phys. Z.*, **17**, 557 and 583 (1916).

25) "CRC Handbook of Chemistry and Physics," 63rd ed, CRC Press, Boca Raton (1982/1983).
